

# Corrective Diffusion Language Models

Shuibai Zhang<sup>1</sup> Fred Zhangzhi Peng<sup>2</sup> Yiheng Zhang<sup>1</sup> Jin Pan<sup>1</sup> Grigoris G Chrysos<sup>1</sup>

## Abstract

While Diffusion Language Models (DLMs) are theoretically well-suited for iterative refinement due to their non-causal structure, they often fail to reliably revise incorrect tokens in practice. The key challenge lies in the model’s inability to distinguish between correct and erroneous tokens in a visible sequence. Standard masked diffusion language model (MDLM) training is restricted to the objective of unmasking, undermining the effectiveness of refinement guided by confidence. Based on this observation, we study *corrective behavior* in DLMs, defined as the ability to assign lower confidence to incorrect tokens and iteratively refine them while preserving correct content. We show that this capability is not induced by conventional masked diffusion objectives and propose a post-training principle oriented by correction that explicitly supervises visible incorrect tokens, enabling discriminative confidence and targeted refinement. To evaluate corrective behavior, we introduce the Code Revision Benchmark, a controllable and executable benchmark for assessing error localization and in-place correction. Experiments on code revision tasks and parallel decoding scenarios demonstrate that models trained with our approach substantially outperform standard MDLMs, with gains that are most pronounced when parallel decoding introduces substantial uncertainty and iterative refinement becomes essential. Our code is publicly available at <https://github.com/zhangshuibai/CDLM>.

## 1. Introduction

Autoregressive (AR) language models dominate text generation by predicting tokens from left to right (Achiam et al., 2023; Guo et al., 2025a; Comanici et al., 2025; Yang et al., 2025; Grattafiori et al., 2024). Recently, diffusion language

<sup>1</sup>University of Wisconsin–Madison <sup>2</sup>Duke University. Correspondence to: Shuibai Zhang <[shuibai@cs.wisc.edu](mailto:shuibai@cs.wisc.edu)>.

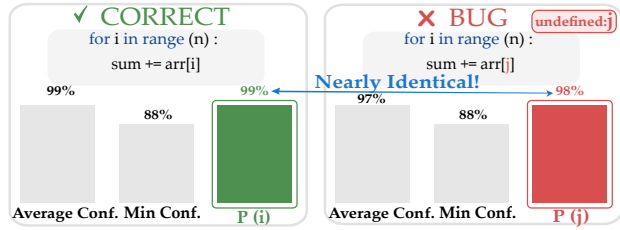


Figure 1. An illustrative example in which the model is **equally confident** in the correct variable (i) and the undefined bug (j). Global metrics (Average/Min) fail to detect this failure mode.

models (DLMs) have emerged as a structurally distinct alternative, replacing causal generation with an iterative denoising process over complete sequences (Nie et al., 2025; Ye et al., 2025; Labs et al., 2025; Song et al., 2025; Zhu et al., 2025). This non-causal formulation decouples token predictions across positions and enables parallel generation (Kang et al., 2025). Beyond differences in sampling efficiency and generation dynamics, this structural distinction endows DLMs with a capability that AR models fundamentally lack: the ability to directly refine an existing sequence through localized, iterative revisions (Wang et al., 2025a; Peng et al., 2025a). Because arbitrary positions can be modified without regenerating the entire context, DLMs are naturally suited for correcting errors in place and progressively improving a complete input. In AR models, later predictions are conditioned on earlier outputs due to causal dependency, restricting an earlier-occurred error from being regenerated when the model propagates forward. This sequential dependency lacks the mechanism for in-place correction. In contrast, DLMs decouple predictions across positions, enabling targeted refinement beyond left-to-right generation.

Despite this structural advantage, standard masked diffusion language models (MDLMs) do not reliably exhibit effective refinement behavior. Under the conventional masked-diffusion objective, supervision is only applied to masked positions. This lack of a learning signal for unmasked positions prevents the model from developing the ability to identify or correct existing errors, as shown in Figure 1. As a result, the model offers limited guidance on where edits are needed during iterative refinement. To formalize this gap, we introduce the notion of *corrective behavior*: the

ability of a model to identify unreliable tokens in a full sequence containing errors, and iteratively refine them while preserving correct content. This capability is essential for effective refinement but is not induced by standard MDLM training objectives.

A key challenge in studying refinement is the absence of a controlled and executable benchmark that directly evaluates such behavior. Most existing evaluations are built around prefix-based completion, which is defined as models generating sequences from a given prefix, a setting tailored to AR models and their left-to-right generation process (Du et al., 2024; Austin et al., 2021b; Liu et al., 2023). These evaluations do not assess whether a model can localize and fix errors in a complete input, which is the core requirement of refinement. A suitable refinement benchmark must allow precise control over corruption type and severity and provide reliable feedback on whether a proposed correction is valid. These considerations motivate the development of both an appropriate benchmark and a post-training principle that equips MDLMs with error-aware, targeted refinement capabilities. We refer to MDLMs that exhibit such corrective behavior as *Corrective Diffusion Language Models (CDLMs)*.

**Our contributions.** In this work, we make the following contributions:

- **A controllable and executable refinement benchmark.** We introduce the **Code Revision Benchmark (CRB)**, constructed by applying type-preserving corruptions of controllable difficulty to real, executable code snippets. CRB enables systematic evaluation of error localization to identify unreliable tokens and iterative refinement, a cyclic process of improving to revise the detected tokens through regeneration, with each instance graded through deterministic execution, to ensure a verifiable output is maintained in a specific input and initial state.
- **A post-training principle for obtaining Corrective Diffusion Language Models (CDLMs).** We revisit the absorbing-uniform mixture objective from the perspective of targeted correction, and show that it provides the missing supervision needed for MDLMs to recognize incorrect tokens and prioritize edits. By explicitly supervising visible corrupted tokens alongside masked reconstruction, this principle induces error-aware confidence and enables reliable, targeted refinement.
- **Improved generation under high uncertainty through corrective ability.** CDLMs improve generation performance in from-scratch code generation and high-uncertainty decoding settings. Compared to standard MDLMs, CDLMs achieve higher accuracy

and benefit more from iterative remasking, demonstrating that correction-aware training enhances generation quality beyond explicit revision.

## 2. Background

### 2.1. Masked Diffusion Language Models

Let  $\mathbf{x} = (x_1, \dots, x_n)$  be a clean token sequence over a vocabulary  $\mathcal{V}$ , and let  $m \in \mathcal{V}$  denote a designated absorbing mask token. We focus on *masked diffusion language models* (MDLMs) (Sahoo et al., 2024), a widely used class of DLMs based on an absorbing corruption process, where tokens are gradually replaced with a masked token until all tokens are masked during training. (Nie et al., 2025; Ye et al., 2025; Labs et al., 2025; Song et al., 2025; Zhu et al., 2025).

**Forward (noising) process** For each training example, a mask ratio  $\lambda \sim \text{Uniform}[0, 1]$  is sampled, and the corrupted sequence  $\mathbf{z}$  is drawn as

$$q_\lambda(\mathbf{z} \mid \mathbf{x}) = \prod_{i=1}^n \begin{cases} \lambda, & z_i = m, \\ 1 - \lambda, & z_i = x_i. \end{cases}$$

**Reverse (denoising) model.** A Transformer parameterizes the conditional distribution  $p_\theta(\mathbf{x} \mid \mathbf{z})$  and is trained using a masked-token reconstruction objective,

$$\mathcal{L}_{\text{absorb}}(\theta) = \mathbb{E}_{\mathbf{x} \sim \mathcal{D}, \mathbf{z} \sim q_\lambda(\cdot \mid \mathbf{x})} \left[ - \sum_{i: z_i = m} \log p_\theta(x_i \mid \mathbf{z}) \right].$$

Only positions with  $z_i = m$  contribute to the loss, while logits at all non-masked positions are ignored.

### 2.2. Confidence-Based Iterative Refinement

DLMs refine sequences by iteratively predicting token-level distributions and selectively remasking uncertain positions (Peng et al., 2025a; Wang et al., 2025a; Kim et al., 2025). Given the current sequence  $\mathbf{z}^{(t)}$ , the model produces a conditional token-level distribution  $p_\theta(\cdot \mid \mathbf{z}^{(t)})$ . From this distribution, we extract both the token prediction and its associated confidence:

$$\hat{x}_i^{(t)} = \arg \max_{v \in \mathcal{V}} p_\theta(v \mid \mathbf{z}^{(t)}), \quad c_i^{(t)} = \max_{v \in \mathcal{V}} p_\theta(v \mid \mathbf{z}^{(t)}).$$

Confidence-based refinement then identifies positions whose confidence falls below a predefined threshold  $\tau$ ,

$$r^{(t)} = \{ i \mid c_i^{(t)} < \tau \},$$

and constructs the next iteration via a unified update rule:

$$z_i^{(t+1)} = \begin{cases} m, & i \in r^{(t)}, \\ \hat{x}_i^{(t)}, & \text{otherwise.} \end{cases}$$

This approach aims to focus edits on positions deemed unreliable by the model, as determined by token-level confidence estimates.

### 3. Code Revision Benchmark (CRB)

Both AR models and DLMs are commonly evaluated through prefix-based completion (Nie et al., 2025; Song et al., 2025; Ni et al., 2025), which does not assess their ability to localize and correct errors in a complete input sequence. A systematic evaluation of refinement behavior instead requires controlled variation of error types, fine-grained control over corruption severity, and deterministic verification of correctness. Code provides an ideal testbed for such evaluation, as program behavior is executable and correctness can be checked deterministically. Building on widely used code-generation benchmarks, including HumanEval (Chen et al., 2021) and MBPP (Austin et al., 2021b) and their extended variants HumanEval+ and MBPP+ (Liu et al., 2023), we introduce the *Code Revision Benchmark (CRB)*. CRB leverages these established datasets while introducing controlled, localized corruptions to enable systematic analysis of error localization and iterative, in-place correction.

#### 3.1. Task Definition

Let  $\mathbf{x}^* = (x_1^*, \dots, x_n^*)$  denote a canonical program represented as a sequence of  $n$  tokens drawn from a vocabulary  $\mathcal{V}$ . CRB introduces errors by selecting an index set  $E \subseteq \{1, \dots, n\}$  and applying a type-preserving replacement operator,

$$z_i^{(0)} = \begin{cases} \phi(x_i^*), & i \in E, \\ x_i^*, & \text{otherwise.} \end{cases}$$

The operator  $\phi(\cdot)$  replaces a token with another token from the same lexical category while preserving token length under the tokenizer.

#### 3.2. Corruption Types

As shown in Figure 2, CRB includes three categories of token-level corruption:

- **Operator substitutions.** An operator token is replaced using a predefined set  $\mathcal{O} = \{+, -, *, /, \%, <, >, <=, >=, ==, !=\}$ .
- **Identifier substitutions.** A token belonging to the identifier class is replaced with another identifier that appears within the same scope of the program. This class includes variable names, function names, and language-defined identifiers such as `True` or `False`. Such substitutions often induce subtle semantic inconsistencies.

#### Canonical Solution

```
def is_prime(n):
    """Return true if a given number is prime,
    and false otherwise."""
    if n < 2:
        return False
    for k in range(2, n - 1):
        if n % k == 0:
            return False
    return True
```

<b>Operator:</b> if n <code>%</code> k == 0 $\downarrow$ if n <code>+</code> k == 0	<b>Identifier:</b> return <code>False</code> $\downarrow$ return <code>True</code>
<b>Literal:</b> if n < 2: $\downarrow$ if n < 0:	

Figure 2. CRB corruption pipeline. A canonical program is tokenized, corrupted via type-preserving token replacement, validated by execution, categorized, and generated as a benchmark instance.

- **Literal substitutions.** Numeric or boolean literals are replaced with others of the same type, introducing incorrect boundary conditions or erroneous behaviors.

#### 3.3. Difficulty Control via Number of Replacements

The corruption severity is controlled by the number of modified positions  $|E|$ . The case  $|E| = 1$  corresponds to a single-error setting with a localized refinement target. Larger values  $|E| > 1$  create multi-error scenarios that require co-ordinated edits and expose the model’s ability to perform multi-step correction. This explicit control over difficulty is essential for analyzing refinement behavior across progressively challenging settings.

#### 3.4. Executable Validation and Instance Construction

Not all type-preserving corruptions necessarily introduce actual errors: in some cases, a modified program may remain semantically correct and pass all tests. To ensure that every CRB instance contains a genuine syntactic or semantic fault with deterministic supervision, we perform executable validation after corruption. Following corruption, the modified program  $z^{(0)}$  is executed using a deterministic grader:

$$\text{Tests}(z^{(0)}) = \begin{cases} \text{pass,} & \text{discard the sample,} \\ \text{fail,} & \text{accept as a CRB instance.} \end{cases}$$

Only programs that fail the tests are retained. This procedure guarantees that every CRB instance contains an actual syntactic or semantic error. The resulting dataset provides controlled, type-preserving corruptions together with deterministic correctness signals, enabling reliable evaluation of both error localization and iterative refinement.

### 4. Conventional Confidence-Based Corrective Behavior in DLMs

To motivate our study of *corrective behavior* in existing DLMs on code error correction, we evaluate several publicly available DLMs on CRB, including LLaDA-8B-Base (Nie et al., 2025), Dream-7B-Base (Ye et al., 2025), and

Table 1. Evaluation of confidence quality (top block) and iterative correction performance (bottom block) under varying numbers of corrupted tokens  $n_{\text{replace}}$ . The top block reports the confidence gap between clean and erroneous tokens ( $gap$ ), together with top-1 and top-5 hit rates measuring how often error tokens appear among the lowest-confidence positions. The bottom block reports Pass@1 after applying confidence-threshold-based iterative refinement for  $T \in \{1, 2, 4\}$  refinement steps.

Model	$n_{\text{replace}} = 1$			$n_{\text{replace}} = 2$			$n_{\text{replace}} = 3$			$n_{\text{replace}} = 4$			$n_{\text{replace}} = 5$		
	gap	top-1	top-5												
Dream-7B-Base	0.578	0.094	0.590	0.536	0.084	0.614	0.528	0.084	0.597	0.528	0.088	0.600	0.529	0.076	0.571
LLaDA-8B-Base	0.235	0.178	0.770	0.209	0.198	0.801	0.199	0.172	0.811	0.185	0.159	0.784	0.191	0.162	0.833
Open-dCoder-0.5B	0.106	0.147	0.509	0.100	0.222	0.655	0.085	0.243	0.701	0.089	0.325	0.759	0.093	0.348	0.795

Model	$n_{\text{replace}} = 1$			$n_{\text{replace}} = 2$			$n_{\text{replace}} = 3$			$n_{\text{replace}} = 4$			$n_{\text{replace}} = 5$		
	T=1	T=2	T=4												
Dream-7B-Base	0.776	0.745	0.732	0.704	0.695	0.686	0.663	0.670	0.673	0.654	0.682	0.683	0.630	0.653	0.644
LLaDA-8B-Base	0.552	0.587	0.596	0.419	0.466	0.483	0.338	0.405	0.421	0.319	0.374	0.407	0.280	0.327	0.359
Open-dCoder-0.5B	0.143	0.230	0.251	0.059	0.162	0.178	0.036	0.116	0.141	0.017	0.089	0.104	0.005	0.061	0.074

Open-dCoder-0.5B (Peng et al., 2025b). Our analysis focuses on two complementary aspects of corrective behavior: (i) the ability to identify erroneous tokens within a complete input, and (ii) the ability to correct such errors through iterative, in-place refinement. All evaluations follow each model’s standard masked-diffusion decoding procedure, using the confidence-threshold-based refinement described in Section 2.2. Models are tested across multiple difficulty levels by varying both the number of corrupted tokens  $|E|$  and the error type.

#### 4.1. Error-Token Identification Performance

We first evaluate whether DLMs can identify erroneous tokens based on their token-level confidence scores at the initial refinement step. Given a corrupted program with error positions  $E \subseteq \{1, \dots, n\}$ , the model assigns each position a confidence score

$$c_i = \max_{v \in \mathcal{V}} p_\theta(v \mid \mathbf{x}),$$

and we examine how well these scores align with the presence of errors. We report two complementary metrics that capture different aspects of error-token identification.

**Confidence Gap.** The confidence gap measures the average difference between confidence assigned to clean positions and that assigned to erroneous positions:

$$\text{Gap} = \mathbb{E}_{i \notin E}[c_i] - \mathbb{E}_{i \in E}[c_i].$$

A larger positive gap indicates that the model assigns systematically lower confidence to erroneous tokens than to clean ones. This metric reflects the degree to which the model’s confidence is calibrated with respect to token-level correctness.

**Top- $K$  Hit Rate.** For a fixed  $K$ , the Top- $K$  set consists of the  $K$  positions with the lowest confidence scores. The

hit rate is defined as

$$\text{Hit}@K = \mathbb{I}(E \cap \text{TopK}(c) \neq \emptyset).$$

This metric measures whether at least one true error is ranked among the most uncertain positions. It captures the model’s ability to prioritize error tokens when refinement is restricted to a small set of candidate locations.

**Results.** In this experiment, we use the standard DLMs with their default configurations. Table 1 summarizes error-token identification performance across increasing corruption severity. Across all models, the confidence gap between clean and erroneous tokens remains limited, with particularly weak separation for Open-dCoder-0.5B. Even in the single-error setting, erroneous tokens often receive confidence values comparable to those of clean tokens. Top- $K$  hit rates show that while erroneous tokens tend to fall within a low-confidence region, they are rarely ranked as the most uncertain positions, as reflected by consistently low Top-1 but higher Top-5 hit rates. Together, these results indicate that token-level confidence in standard MDLMs is only coarsely aligned with correctness and lacks the resolution required for precise error localization. As a result, confidence-based ranking alone is insufficient to reliably identify error tokens, limiting its effectiveness for targeted, in-place refinement.

#### 4.2. Error-Correction Ability via Iterative Refinement

We next evaluate whether DLMs can repair corrupted programs through iterative, in-place refinement. At each refinement step  $t$ , the model selectively remasks a subset of positions and re-predicts their values based on token-level confidence scores. Let  $c_i^{(t)}$  denote the confidence assigned to token  $i$  after step  $t$ .

**Iterative Refinement.** We follow the confidence-threshold-based refinement protocol introduced in

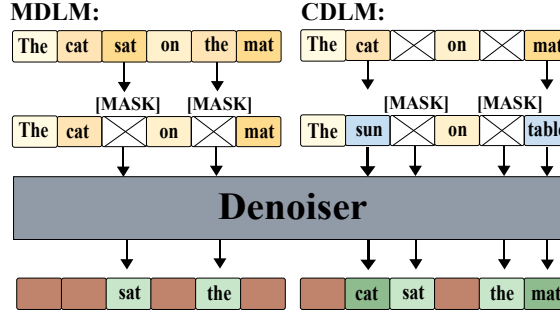


Figure 3. Comparison of training supervision in MDLM and CDLM and its implication for corrective behavior. Cross-marked boxes denote masked tokens, and beige boxes denote visible inputs. Standard MDLMs apply supervision only to masked tokens, leaving visible tokens unsupervised even when incorrect. CDLM explicitly supervises corrupted visible tokens and encourages lower confidence on unreliable content. This supervision difference enables error-aware confidence and targeted, in-place correction during iterative refinement.

Section 2.2. Given a fixed threshold  $\tau$ , all positions whose confidence falls below the threshold are remasked at step  $t$ :

$$r^{(t)} = \{ i : c_i^{(t)} < \tau \}.$$

Unless otherwise specified, we set  $\tau = 0.9$  in all experiments, as this value provides a good balance between stability and flexibility in practice. This dynamic strategy allows the remasking set to adapt to the model’s evolving uncertainty across refinement steps.

**Pass@1 Metric.** After  $T$  refinement steps, the final program is executed using an external grader. Pass@1 is defined as the fraction of programs that execute successfully and produce the correct output:

$$\text{Pass@1} = \mathbb{I}(\text{grader}(x^{(T)}) = \text{correct}).$$

**Results.** Table 1 reports Pass@1 after confidence-threshold-based iterative refinement. Across all models and corruption levels, error-correction performance remains limited, even in the single-error setting. Although Dream-7B-Base performs best, followed by LLaDA-8B-Base and Open-dCoder-0.5B, all models fail to correct a substantial fraction of programs, indicating that targeted correction is challenging for standard DLMs. Increasing the number of refinement steps yields only marginal and inconsistent gains, which is consistent with the weak error-token identification observed in Section 4.1. Because low-confidence positions do not reliably correspond to true errors, iterative remasking often overwrites correct tokens while leaving actual errors unresolved, limiting the effectiveness of additional refinement steps.

## 5. Towards Corrective Behavior

Standard MDLMs trained with the absorbing-mask objective often exhibit limited error awareness during refinement. As illustrated in Figure 3, unmasked tokens receive no direct supervision, which limits the model’s ability to learn confidence signals that reflect token-level reliability. As a result, the model struggles to identify where edits are needed, weakening the effectiveness of iterative refinement.

To formalize refinement-oriented DLMs, we introduce the following definition.

*Definition* (Corrective Diffusion Language Model). A *Corrective Diffusion Language Model (CDLM)* is a diffusion language model that exhibits *corrective behavior*, namely error-aware refinement. Specifically, a CDLM:

1. assigns systematically lower confidence to erroneous or implausible tokens than to correct ones;
2. leverages confidence signals to localize errors and iteratively improve sequence correctness under iterative refinement.

Together, these properties enable reliable error localization and targeted, in-place correction during diffusion-based refinement.

To induce such corrective behavior, we propose a correction-aware post-training principle that combines absorbing-mask corruption with uniform replacement corruption. Absorbing corruption preserves standard masked reconstruction, while uniform replacement injects explicit noise into visible positions, explicitly training the model to recognize and downweight incorrect content. By mixing these two corruption processes, the model jointly learns reconstruction and error awareness, resulting in better calibrated token-level confidence and more reliable, targeted refinement.

Concretely, given a clean sequence  $\mathbf{x}^* = (x_1^*, \dots, x_n^*)$ , we apply a two-stage corruption process. First, a randomly selected subset of tokens is masked using the standard absorbing-mask mechanism, providing reconstruction targets as in MDLMs. Second, among the remaining visible tokens, each token is independently replaced with a uniformly sampled incorrect but still visible token with probability  $\alpha \in (0, 1)$ , where  $\alpha$  denotes the mixture probability. This construction introduces both missing content that must be reconstructed and unreliable visible content that must be identified as incorrect.

Let  $\mathcal{M}$  denote the set of masked positions and  $\mathcal{V}$  the set of visible (unmasked) positions. For each visible position  $i \in \mathcal{V}$ , we sample a Bernoulli random variable  $z_i \sim \text{Bernoulli}(\alpha)$ , where  $z_i = 1$  indicates that position  $i$  is corrupted via uniform replacement. We train the model

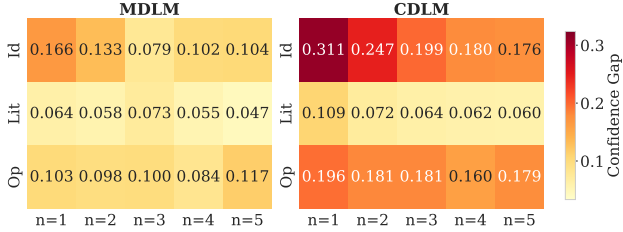


Figure 4. Confidence gap between clean and corrupted tokens for MDLM and CDLM across error types and numbers of replacements on the HumanEval dataset. Error types include identifier substitutions (Id), literal substitutions (Lit), and operator substitutions (Op). Larger values reflect stronger separation and improved error-awareness, with CDLM showing consistently higher gaps than MDLM.

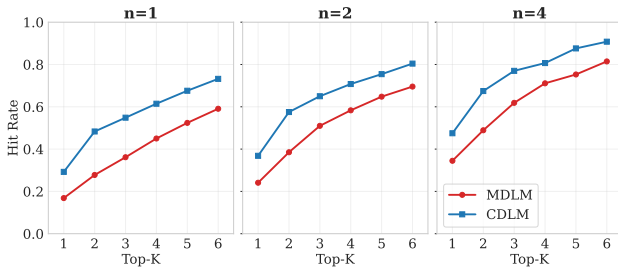


Figure 5. Top- $K$  hit rate of identifying at least one true error among the  $K$  lowest-confidence positions for MDLM and CDLM on the HumanEval dataset. Higher values indicate more reliable error localization, with CDLM consistently outperforming MDLM across different numbers of corrupted tokens.

using the following mixture objective:

$$\mathcal{L} = \mathbb{E}_{\text{corruption}} \left[ \frac{1}{|\mathcal{M}|} \sum_{i \in \mathcal{M}} \ell_i + \lambda_{\text{noise}} \sum_{i \in \mathcal{V}} z_i \ell_i \right], \quad (1)$$

where  $\ell_i$  denotes the per-token cross-entropy loss. The expectation is taken over the stochastic corruption process, including both mask sampling and uniform replacement.

The first term preserves the standard denoising capability of MDLMs. The second term introduces explicit supervision on incorrect but visible tokens whenever uniform replacement is applied, encouraging the model to assign lower confidence to unreliable content.

Related work such as Generalized Interpolating Discrete Diffusion (von Rütte et al., 2025) also combines absorbing and uniform noise corruption, but is primarily motivated by improving general generation quality. In contrast, our work adopts the masked diffusion paradigm and focuses on inducing corrective behavior under localized, iterative refinement. Implementation details of the corruption process and a more detailed comparison are provided in Appendix G.1.

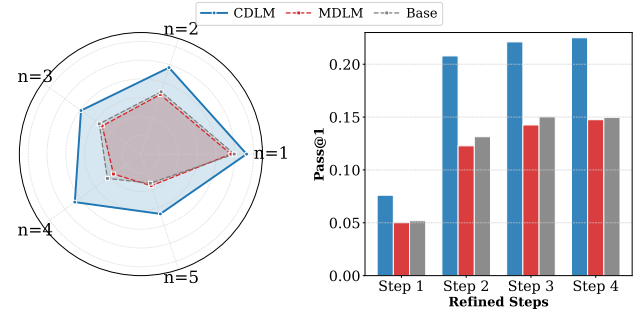


Figure 6. Pass@1 performance for MDLM, CDLM, and the base model under dynamic confidence-based refinement on the HumanEval dataset. Left: Pass@1 after four refinement steps with confidence threshold 0.9, shown across different numbers of corrupted tokens. Right: Mean Pass@1 averaged over all error types and corruption levels as the refinement depth increases. CDLM consistently outperforms MDLM and the base model under all settings.

## 6. Experiments

We evaluate the proposed absorbing–uniform mixture objective on CRB. Unless otherwise noted, our default model is CDLM-0.5B, obtained by finetuning the OPEN-DCODER-0.5B (Peng et al., 2025b) checkpoint for 2000 steps on the Nemotron coding corpus (NVIDIA et al., 2025). We compare three models throughout this section: (i) the pre-trained base model, (ii) the absorbing-only objective finetuned model, and (iii) the mixture-trained CDLM-0.5B. Training settings are identical across (ii) and (iii) except for the choice of objective.

### 6.1. How the Mixture Objective Improves Error Localization and Correction

We ablate the effect of training objective by comparing the absorbing-only model with the mixture-trained CDLM-0.5B. Both models use the same dataset, optimizer, learning rate schedule, and number of training steps. This isolates the effect of the mixture objective itself.

**Error Localization Improvements.** Error-token identification is evaluated using confidence gap and Top- $K$  hit rate. Figure 4 reports the average confidence gap between clean and erroneous tokens across CRB difficulty levels. The mixture objective produces substantially larger gaps compared to both the base model and the absorbing-only model, indicating that CDLM-0.5B assigns meaningfully lower confidence to incorrect tokens. Figure 5 reports the Top- $K$  hit rate for  $K \in \{1, \dots, 6\}$  across different numbers of corrupted tokens. Across all settings, CDLM consistently achieves higher hit rates than both the absorbing-only objective finetuned MDLM and the untrained base model. The advantage is particularly clear at small  $K$ , where correctly identifying at least one true error is most challenging. As

$K$  increases, the gap remains stable, indicating that the mixture objective produces confidence scores that more reliably prioritize erroneous tokens.

**Error Correction Improvements.** We evaluate end-to-end correction ability using deterministic Pass@1 under dynamic-confidence refinement. Figure 6 summarizes performance across corruption levels and refinement depths. Across increasing corruption severity  $n_{\text{replace}} \in \{1, \dots, 5\}$ , CDLM consistently achieves higher Pass@1 than both the absorbing-only finetuned MDLM and the untrained base model, indicating more reliable correction even when multiple errors must be revised. When averaging over all error types and corruption levels, CDLM further exhibits steady gains as refinement depth increases and maintains a consistent margin over the absorbing-only objective. Aggregated Pass@1 results across all CRB settings can be found in Appendix C, confirming a substantial improvement from mixture training over both absorbing-only finetuning and the base model.

## 6.2. Ablation Studies

**Effect of Mixture Probability.** We analyze the effect of the mixture probability  $\alpha$ , which controls the fraction of clean tokens replaced by uniformly sampled noise during training. This ablation is conducted using Open-dCoder-0.5B, where we train 10 models with different values of  $\alpha$  while keeping all other hyperparameters fixed. Figure 7 summarizes its impact on confidence separation, error localization, and end-to-end correction.

As  $\alpha$  increases, the confidence gap between clean and erroneous tokens consistently grows (Figure 7a), indicating improved average separation between reliable and unreliable tokens. However, this improvement does not translate monotonically to error localization. When  $\alpha$  exceeds approximately 0.7, the Top-5 hit rate declines (Figure 7b) while the Top-5 false positive rate increases (Figure 7c), suggesting that excessive uniform corruption degrades contextual signal and causes some clean tokens to be assigned low confidence. This tradeoff is also reflected in end-to-end correction. As shown in Figure 7d, Pass@1 initially improves with increasing  $\alpha$  but drops once the probability becomes too large. Overall, these results indicate that while uniform replacement supervision strengthens confidence separation, overly aggressive corruption impairs contextual understanding and reduces error localization precision, highlighting the need for a balanced mixture probability.

## 7. When Correction-Aware Training Helps Generation

We analyze the conditions under which the proposed mixture objective improves generation performance. In partic-

Table 2. From-scratch code generation results on HumanEval and HumanEval+. CDLM consistently achieves higher Pass@1 and Pass@10 across decoding strategies. Results on MBPP and MBPP+ are reported in Appendix E.1.

Method	HumanEval		HumanEval+	
	Pass@1	Pass@10	Pass@1	Pass@10
MDLM (Vanilla)	0.19	0.38	0.17	0.34
CDLM (Vanilla)	<b>0.22</b>	<b>0.42</b>	<b>0.21</b>	<b>0.39</b>
Base (Vanilla)	0.19	0.37	0.17	0.32
MDLM (ReMDM)	0.20	0.38	0.17	0.34
CDLM (ReMDM)	<b>0.21</b>	<b>0.43</b>	<b>0.20</b>	<b>0.38</b>
Base (ReMDM)	0.18	0.33	0.16	0.29

Table 3. Per-task and grouped average accuracy of LLADA-2.0-MINI (Bie et al., 2025) on ParallelBench (Kang et al., 2025) under confidence-based decoding. Each entry reports *Fixed* / *Remask* accuracy, where *Fixed* denotes decoding without remasking and *Remask* enables iterative token refinement. Bold numbers indicate the best performance within each row.

Task	Base	MDLM		CDLM	
		Fixed / Remask		Fixed / Remask	
<b>Low-Entropy</b>					
Copy	0.97 / 0.97	<b>1.00</b>	<b>1.00</b>	<b>1.00</b>	<b>1.00</b>
Reverse	0.60 / 0.63	<b>1.00</b>	<b>1.00</b>	<b>1.00</b>	<b>1.00</b>
Sort	0.15 / 0.19	0.61 / 0.61	0.60	<b>0.64</b>	
Insert Index	0.23 / 0.24	<b>1.00</b>	<b>1.00</b>	0.99 / 0.99	
Remove Index	0.36 / 0.37	<b>1.00</b>	<b>1.00</b>	<b>1.00</b>	<b>1.00</b>
Replace Index	0.41 / 0.41	<b>1.00</b>	<b>1.00</b>	<b>1.00</b>	<b>1.00</b>
<b>Average (Low)</b>	0.45 / 0.47	0.93 / 0.93	0.93	<b>0.94</b>	
<b>High-Entropy</b>					
Shuffle	0.37 / 0.52	0.47 / 0.38	0.45	<b>0.64</b>	
Insert Random	0.23 / 0.35	0.40 / 0.44	0.40	<b>0.72</b>	
Remove Random	0.65 / 0.70	0.75 / 0.72	0.69	<b>0.77</b>	
Replace Random	0.51 / 0.67	0.25 / 0.26	0.30	<b>0.37</b>	
<b>Average (High)</b>	0.44 / 0.56	0.47 / 0.45	0.46	<b>0.62</b>	
<b>Average (All)</b>	0.45 / 0.50	0.75 / 0.74	0.74	<b>0.81</b>	

ular, we focus on *from-scratch code generation* and high-uncertainty generation regimes that stress parallel decoding and iterative refinement.

## 7.1. From-Scratch Code Generation

We first evaluate our mixture objective in from-scratch code generation, where the full program body (excluding the function signature) is replaced with mask tokens and must be generated entirely by the model. Unlike explicit correction tasks, this setting does not involve identifying injected errors or preserving clean tokens, and instead evaluates general denoising and generation ability under masked generation. All models use the same remask-based decoding strategy (Peng et al., 2025a), where low-confidence tokens are iteratively remasked according to a linear schedule. Table 2 reports Pass@1 and Pass@10 on HumanEval and HumanEval+ (Du

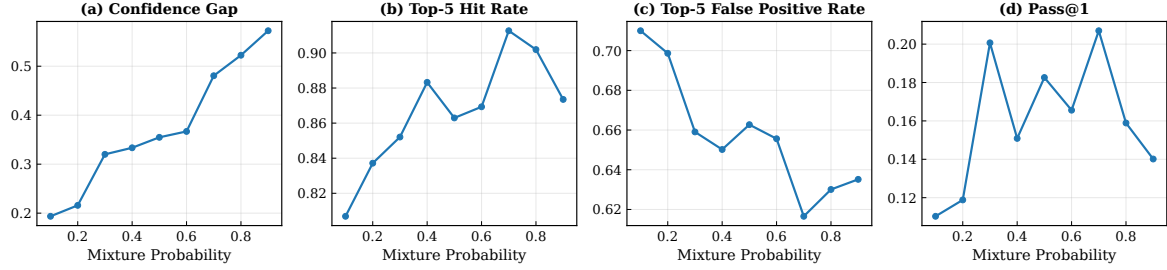


Figure 7. Effect of mixture probability on confidence separation, error localization, and end-to-end correction. (a) Confidence gap between clean and erroneous tokens. (b) Top-5 hit rate for error-token identification. (c) Top-5 false positive rate. (d) Pass@1 under dynamic-confidence refinement. Increasing the mixture probability strengthens average confidence separation but introduces a tradeoff: excessive uniform corruption degrades contextual information, increases false positives, and ultimately reduces correction performance.

et al., 2024; Liu et al., 2023). Across both benchmarks, the mixture objective consistently improves performance relative to the absorbing-only MDLM baseline. Overall, CDLM achieves higher Pass@1 and Pass@10 than both the base model and the absorbing-only finetuned model.

We further evaluate both MDLM and CDLM under the ReMDM decoding strategy of Wang et al. (2025a), which fixes each token’s confidence score at the step when it is first unmasked, in contrast to vanilla confidence-based decoding where confidence is recomputed at every refinement step. The overall trend remains unchanged: under both vanilla and ReMDM remask-based decoding, CDLM consistently outperforms MDLM, indicating that explicit supervision on corrupted tokens also benefits from-scratch generation.

## 7.2. High-Uncertainty Generation and Parallel Decoding

While the benchmarks above focus on from-scratch code generation with relatively well-defined targets, many generation scenarios exhibit substantially higher output uncertainty, where multiple distinct outputs are equally valid. In such regimes, errors arise naturally from parallel decoding, making iterative correction essential. To study this setting, we evaluate our models on ParallelBench (Kang et al., 2025), which stresses parallel decoding under high-entropy output spaces. Both training and evaluation are conducted on ParallelBench using LLADA-2.0-MINI (16B) (Bie et al., 2025). The benchmark consists of structured transformation tasks such as copying, shuffling, and replacement; concrete task definitions and examples are provided in Appendix E. Table 3 reports per-task and averaged accuracy under confidence-based decoding with a low confidence threshold, which increases parallelism and amplifies decoding-induced errors.

ParallelBench tasks can be broadly categorized by their output entropy. *Low-entropy* tasks admit a single valid output for a given input. For example, in the **Copy** task, the model is required to reproduce the input sequence exactly,

leaving no ambiguity in the correct output. In contrast, *high-entropy* tasks admit multiple valid outputs. For instance, in the **Shuffle** task, any permutation of the input sequence that differs from the original order is acceptable, resulting in a large space of equally correct solutions.

For low-entropy tasks, remasking yields limited improvements across all training methods, as errors are less frequent and confidence estimates are more stable. In contrast, for high-entropy tasks, remasking becomes crucial. While the base model benefits moderately from remasking, the absorbing-only MDLM fails to consistently exploit it, and in some cases remasking even degrades performance. We attribute this behavior to poorly calibrated token-level confidence, which prevents remasking from reliably targeting erroneous predictions.

In contrast, CDLM exhibits substantially larger gains from remasking on high-entropy tasks. Under high-entropy settings, the average accuracy improves from 0.47 with the absorbing-only MDLM to 0.62 with CDLM, highlighting a pronounced benefit of the mixture objective when output space has high entropy. By explicitly supervising corrupted but visible tokens, the mixture objective induces more error-aware confidence estimates, enabling effective iterative refinement under high parallelism. Overall, these results demonstrate that correction-aware training improves generation performance beyond explicit revision, particularly in high-uncertainty decoding regimes.

## 8. Conclusion

We demonstrate that standard masked diffusion objectives fail to induce error-aware, token-level confidence, which leads to unreliable iterative refinement. We introduce the Code Revision Benchmark (CRB), a controllable and executable benchmark that isolates error localization and in-place correction from prefix-based generation. We propose a correction-oriented post-training principle based on a mixture of absorbing and uniform corruption that explicitly supervises visible corrupted tokens alongside masked recon-

struction. Models trained with this objective consistently exhibit stronger error awareness, more reliable targeted refinement, and improved performance in correction settings. Beyond explicit revision tasks, we show that correction-aware training substantially improves parallel decoding under high-entropy output regimes, where effective remasking is essential. Together, these results suggest that error-aware training is a promising direction for enabling robust, in-place correction and reliable parallel generation.

## Impact Statement

This work studies training and evaluation methods for diffusion language models to improve error awareness and iterative refinement. While these methods may improve the reliability of generative systems, diffusion language models can still produce incorrect or misleading outputs if deployed without appropriate safeguards.

## References

Achiam, J., Adler, S., Agarwal, S., Ahmad, L., Akkaya, I., Aleman, F. L., Almeida, D., Altenschmidt, J., Altman, S., Anadkat, S., et al. Gpt-4 technical report. *arXiv preprint arXiv:2303.08774*, 2023.

Arriola, M., Sahoo, S. S., Gokaslan, A., Yang, Z., Qi, Z., Han, J., Chiu, J. T., and Kuleshov, V. Block diffusion: Interpolating between autoregressive and diffusion language models. In *The Thirteenth International Conference on Learning Representations*, 2025. URL <https://openreview.net/forum?id=tyEyYT267x>.

Austin, J., Johnson, D. D., Ho, J., Tarlow, D., and van den Berg, R. Structured denoising diffusion models in discrete state-spaces. In Beygelzimer, A., Dauphin, Y., Liang, P., and Vaughan, J. W. (eds.), *Advances in Neural Information Processing Systems*, 2021a. URL <https://openreview.net/forum?id=h7-XixPCAL>.

Austin, J., Odena, A., Nye, M., Bosma, M., Michalewski, H., Dohan, D., Jiang, E., Cai, C., Terry, M., Le, Q., et al. Program synthesis with large language models. *arXiv preprint arXiv:2108.07732*, 2021b.

Bie, T., Cao, M., Chen, K., Du, L., Gong, M., Gong, Z., Gu, Y., Hu, J., Huang, Z., Lan, Z., Li, C., Li, C., Li, J., Li, Z., Liu, H., Liu, L., Lu, G., Lu, X., Ma, Y., Tan, J., Wei, L., Wen, J.-R., Xing, Y., Zhang, X., Zhao, J., Zheng, D., Zhou, J., Zhou, J., Zhou, Z., Zhu, L., and Zhuang, Y. Llada2.0: Scaling up diffusion language models to 100b, 2025. URL <https://arxiv.org/abs/2512.15745>.

Chao, C.-H., Sun, W.-F., Liang, H., Lee, C.-Y., and Krishnan, R. G. Beyond masked and unmasked: Discrete diffusion models via partial masking, 2025. URL <https://arxiv.org/abs/2505.18495>.

Chen, M., Tworek, J., Jun, H., Yuan, Q., de Oliveira Pinto, H. P., Kaplan, J., Edwards, H., Burda, Y., Joseph, N., Brockman, G., Ray, A., Puri, R., Krueger, G., Petrov, M., Khlaaf, H., Sastry, G., Mishkin, P., Chan, B., Gray, S., Ryder, N., Pavlov, M., Power, A., Kaiser, L., Bavarian, M., Winter, C., Tillet, P., Such, F. P., Cummings, D., Plappert, M., Chantzis, F., Barnes, E., Herbert-Voss, A., Guss, W. H., Nichol, A., Paino, A., Tezak, N., Tang, J., Babuschkin, I., Balaji, S., Jain, S., Saunders, W., Hesse, C., Carr, A. N., Leike, J., Achiam, J., Misra, V., Morikawa, E., Radford, A., Knight, M., Brundage, M., Murati, M., Mayer, K., Welinder, P., McGrew, B., Amodei, D., McCandlish, S., Sutskever, I., and Zaremba, W. Evaluating large language models trained on code, 2021. URL <https://arxiv.org/abs/2107.03374>.

Chen, S., Cong, K., and Li, J. Optimal inference schedules for masked diffusion models. *arXiv preprint arXiv:2511.04647*, 2025.

Chi, W., Chen, V., Shar, R., Mittal, A., Liang, J., Chiang, W.-L., Angelopoulos, A. N., Stoica, I., Neubig, G., Talwalkar, A., and Donahue, C. Edit-bench: Evaluating llm abilities to perform real-world instructed code edits, 2025. URL <https://arxiv.org/abs/2511.04486>.

Comanici, G., Bieber, E., Schaeckermann, M., Pasupat, I., Sachdeva, N., Dhillon, I., Blistein, M., Ram, O., Zhang, D., Rosen, E., et al. Gemini 2.5: Pushing the frontier with advanced reasoning, multimodality, long context, and next generation agentic capabilities. *arXiv preprint arXiv:2507.06261*, 2025.

Du, X., Liu, M., Wang, K., Wang, H., Liu, J., Chen, Y., Feng, J., Sha, C., Peng, X., and Lou, Y. Evaluating large language models in class-level code generation. In *Proceedings of the IEEE/ACM 46th International Conference on Software Engineering*, ICSE '24, New York, NY, USA, 2024. Association for Computing Machinery. ISBN 9798400702174. doi: 10.1145/3597503.3639219. URL <https://doi.org/10.1145/3597503.3639219>.

Gao, Y., Ji, Z., Wang, Y., Qi, B., Xu, H., and Zhang, L. Self speculative decoding for diffusion large language models, 2025. URL <https://arxiv.org/abs/2510.04147>.

Gratiafiori, A., Dubey, A., Jauhri, A., Pandey, A., Kadian, A., Al-Dahle, A., Letman, A., Mathur, A., Schelten, A., Vaughan, A., Yang, A., Fan, A., Goyal, A., Hartshorn, A., Yang, A., Mitra, A., Sravankumar, A., Korenev, A., Hinsvark, A., Rao, A., Zhang, A., Rodriguez, A.,

Gregerson, A., Spataru, A., Roziere, B., Biron, B., Tang, B., Chern, B., Caucheteux, C., Nayak, C., Bi, C., Marra, C., McConnell, C., Keller, C., Touret, C., Wu, C., Wong, C., Ferrer, C. C., Nikolaidis, C., Allonsius, D., Song, D., Pintz, D., Livshits, D., Wyatt, D., Esiobu, D., Choudhary, D., Mahajan, D., Garcia-Olano, D., Perino, D., Hupkes, D., Lakomkin, E., AlBadawy, E., Lobanova, E., Dinan, E., Smith, E. M., Radenovic, F., Guzmán, F., Zhang, F., Synnaeve, G., Lee, G., Anderson, G. L., Thattai, G., Nail, G., Mialon, G., Pang, G., Cucurell, G., Nguyen, H., Kovalvaar, H., Xu, H., Touvron, H., Zarov, I., Ibarra, I. A., Kloumann, I., Misra, I., Evtimov, I., Zhang, J., Copet, J., Lee, J., Geffert, J., Vranes, J., Park, J., Mahadeokar, J., Shah, J., van der Linde, J., Billock, J., Hong, J., Lee, J., Fu, J., Chi, J., Huang, J., Liu, J., Wang, J., Yu, J., Bitton, J., Spisak, J., Park, J., Rocca, J., Johnstun, J., Saxe, J., Jia, J., Alwala, K. V., Prasad, K., Upasani, K., Plawiak, K., Li, K., Heafield, K., Stone, K., El-Arini, K., Iyer, K., Malik, K., Chiu, K., Bhalla, K., Lakhotia, K., Rantala-Yeary, L., van der Maaten, L., Chen, L., Tan, L., Jenkins, L., Martin, L., Madaan, L., Malo, L., Blecher, L., Landzaat, L., de Oliveira, L., Muzzi, M., Pasupuleti, M., Singh, M., Paluri, M., Kardas, M., Tsimpoukelli, M., Oldham, M., Rita, M., Pavlova, M., Kambadur, M., Lewis, M., Si, M., Singh, M. K., Hassan, M., Goyal, N., Torabi, N., Bashlykov, N., Bogoychev, N., Chatterji, N., Zhang, N., Duchenne, O., Çelebi, O., Alrassy, P., Zhang, P., Li, P., Vasic, P., Weng, P., Bhargava, P., Dubal, P., Krishnan, P., Koura, P. S., Xu, P., He, Q., Dong, Q., Srinivasan, R., Ganapathy, R., Calderer, R., Cabral, R. S., Stojnic, R., Raileanu, R., Maheswari, R., Girdhar, R., Patel, R., Sauvestre, R., Polidoro, R., Sumbaly, R., Taylor, R., Silva, R., Hou, R., Wang, R., Hosseini, S., Chennabasappa, S., Singh, S., Bell, S., Kim, S. S., Edunov, S., Nie, S., Narang, S., Raparthy, S., Shen, S., Wan, S., Bhosale, S., Zhang, S., Vandenhende, S., Batra, S., Whitman, S., Sootla, S., Collot, S., Gururangan, S., Borodinsky, S., Herman, T., Fowler, T., Sheasha, T., Georgiou, T., Scialom, T., Speckbacher, T., Mihaylov, T., Xiao, T., Karn, U., Goswami, V., Gupta, V., Ramanathan, V., Kerkez, V., Gonguet, V., Do, V., Vogeti, V., Albiero, V., Petrovic, V., Chu, W., Xiong, W., Fu, W., Meers, W., Martinet, X., Wang, X., Wang, X., Tan, X. E., Xia, X., Xie, X., Jia, X., Wang, X., Goldschlag, Y., Gaur, Y., Babaei, Y., Wen, Y., Song, Y., Zhang, Y., Li, Y., Mao, Y., Coudert, Z. D., Yan, Z., Chen, Z., Papakipos, Z., Singh, A., Srivastava, A., Jain, A., Kelsey, A., Shajnfeld, A., Gangidi, A., Victoria, A., Goldstand, A., Menon, A., Sharma, A., Boesenberg, A., Baevski, A., Feinstein, A., Kallet, A., Sangani, A., Teo, A., Yunus, A., Lupu, A., Alvarado, A., Caples, A., Gu, A., Ho, A., Poulton, A., Ryan, A., Ramchandani, A., Dong, A., Franco, A., Goyal, A., Saraf, A., Chowdhury, A., Gabriel, A., Bharambe, A., Eisenman, A., Yazdan, A., James, B., Maurer, B., Leonhardi, B., Huang, B., Loyd, B., Paola, B. D., Paranjape, B., Liu, B., Wu, B., Ni, B., Hancock, B., Wasti, B., Spence, B., Stojkovic, B., Gamido, B., Montalvo, B., Parker, C., Burton, C., Mejia, C., Liu, C., Wang, C., Kim, C., Zhou, C., Hu, C., Chu, C.-H., Cai, C., Tindal, C., Feichtenhofer, C., Gao, C., Civin, D., Beaty, D., Kreymer, D., Li, D., Adkins, D., Xu, D., Testuggine, D., David, D., Parikh, D., Liskovich, D., Foss, D., Wang, D., Le, D., Holland, D., Dowling, E., Jamil, E., Montgomery, E., Presani, E., Hahn, E., Wood, E., Le, E.-T., Brinkman, E., Arcaute, E., Dunbar, E., Smothers, E., Sun, F., Kreuk, F., Tian, F., Kokkinos, F., Ozgenel, F., Caggioni, F., Kanayet, F., Seide, F., Florez, G. M., Schwarz, G., Badeer, G., Swee, G., Halpern, G., Herman, G., Sizov, G., Guangyi, Zhang, Lakshminarayanan, G., Inan, H., Shojanazeri, H., Zou, H., Wang, H., Zha, H., Habeeb, H., Rudolph, H., Suk, H., Aspegren, H., Goldman, H., Zhan, H., Damlaj, I., Molybog, I., Tufanov, I., Leontiadis, I., Veliche, I.-E., Gat, I., Weissman, J., Geboski, J., Kohli, J., Lam, J., Asher, J., Gaya, J.-B., Marcus, J., Tang, J., Chan, J., Zhen, J., Reizenstein, J., Teboul, J., Zhong, J., Jin, J., Yang, J., Cummings, J., Carvill, J., Shepard, J., McPhie, J., Torres, J., Ginsburg, J., Wang, J., Wu, K., U, K. H., Saxena, K., Khandelwal, K., Zand, K., Matosich, K., Veeraraghavan, K., Michelena, K., Li, K., Jagadeesh, K., Huang, K., Chawla, K., Huang, K., Chen, L., Garg, L., A. L., Silva, L., Bell, L., Zhang, L., Guo, L., Yu, L., Moshkovich, L., Wehrstedt, L., Khabsa, M., Avalani, M., Bhatt, M., Mankus, M., Hasson, M., Lennie, M., Reso, M., Groshev, M., Naumov, M., Lathi, M., Keneally, M., Liu, M., Seltzer, M. L., Valko, M., Restrepo, M., Patel, M., Vyatskov, M., Samvelyan, M., Clark, M., Macey, M., Wang, M., Hermoso, M. J., Metanat, M., Rastegari, M., Bansal, M., Santhanam, N., Parks, N., White, N., Bawa, N., Singhal, N., Egebo, N., Usunier, N., Mehta, N., Laptev, N. P., Dong, N., Cheng, N., Chernoguz, O., Hart, O., Salpekar, O., Kalinli, O., Kent, P., Parekh, P., Saab, P., Balaji, P., Rittner, P., Bontrager, P., Roux, P., Dollar, P., Zvyagina, P., Ratanchandani, P., Yuvraj, P., Liang, Q., Alao, R., Rodriguez, R., Ayub, R., Murthy, R., Nayani, R., Mitra, R., Parthasarathy, R., Li, R., Hogan, R., Battey, R., Wang, R., Howes, R., Rinott, R., Mehta, S., Siby, S., Bondu, S. J., Datta, S., Chugh, S., Hunt, S., Dhillon, S., Sidorov, S., Pan, S., Mahajan, S., Verma, S., Yamamoto, S., Ramaswamy, S., Lindsay, S., Lindsay, S., Feng, S., Lin, S., Zha, S. C., Patil, S., Shankar, S., Zhang, S., Zhang, S., Wang, S., Agarwal, S., Sajuyigbe, S., Chintala, S., Max, S., Chen, S., Kehoe, S., Satterfield, S., Govindaprasad, S., Gupta, S., Deng, S., Cho, S., Virk, S., Subramanian, S., Choudhury, S., Goldman, S., Remez, T., Glaser, T., Best, T., Koehler, T., Robinson, T., Li, T., Zhang, T., Matthews, T., Chou, T., Shaked, T., Vontimitta, V., Ajayi, V., Montanez, V., Mohan, V., Kumar, V. S., Mangla, V., Ionescu, V., Poenaru, V., Mihailescu, V. T., Ivanov, V., Li, W., Wang, W., Jiang, W.,

Bouaziz, W., Constable, W., Tang, X., Wu, X., Wang, X., Wu, X., Gao, X., Kleinman, Y., Chen, Y., Hu, Y., Jia, Y., Qi, Y., Li, Y., Zhang, Y., Zhang, Y., Adi, Y., Nam, Y., Yu, Wang, Zhao, Y., Hao, Y., Qian, Y., Li, Y., He, Y., Rait, Z., DeVito, Z., Rosnbrick, Z., Wen, Z., Yang, Z., Zhao, Z., and Ma, Z. The llama 3 herd of models, 2024. URL <https://arxiv.org/abs/2407.21783>.

Guo, D., Yang, D., Zhang, H., Song, J., Zhang, R., Xu, R., Zhu, Q., Ma, S., Wang, P., Bi, X., et al. Deepseek-r1: Incentivizing reasoning capability in llms via reinforcement learning. *arXiv preprint arXiv:2501.12948*, 2025a.

Guo, J., Li, Z., Liu, X., Ma, K., Zheng, T., Yu, Z., Pan, D., LI, Y., Liu, R., Wang, Y., Guo, S., Qu, X., Yue, X., Zhang, G., Chen, W., and Fu, J. Codeeditor-bench: Evaluating code editing capability of LLMs. In *ICLR 2025 Third Workshop on Deep Learning for Code*, 2025b. URL <https://openreview.net/forum?id=6yTgoh0J0X>.

Havasi, M., Karrer, B., Gat, I., and Chen, R. T. Q. Edit flows: Variable length discrete flow matching with sequence-level edit operations. In *The Thirty-ninth Annual Conference on Neural Information Processing Systems*, 2025. URL <https://openreview.net/forum?id=FXWwYz1p8a>.

He, Z., Sun, T., Tang, Q., Wang, K., Huang, X., and Qiu, X. DiffusionBERT: Improving generative masked language models with diffusion models. In Rogers, A., Boyd-Graber, J., and Okazaki, N. (eds.), *Proceedings of the 61st Annual Meeting of the Association for Computational Linguistics (Volume 1: Long Papers)*, pp. 4521–4534, Toronto, Canada, July 2023. Association for Computational Linguistics. doi: 10.18653/v1/2023.acl-long.248. URL <https://aclanthology.org/2023.acl-long.248>.

Hu, L., Kou, S., Fu, Y., Rajbhandari, S., Rosing, T., He, Y., Deng, Z., and Zhang, H. Fast and accurate causal parallel decoding using jacobi forcing, 2025. URL <https://arxiv.org/abs/2512.14681>.

Huang, J., Chen, X., Mishra, S., Zheng, H. S., Yu, A. W., Song, X., and Zhou, D. Large language models cannot self-correct reasoning yet. In *The Twelfth International Conference on Learning Representations*, 2024. URL <https://openreview.net/forum?id=1kmD3fKBPQ>.

Israel, D., den Broeck, G. V., and Grover, A. Accelerating diffusion llms via adaptive parallel decoding, 2025. URL <https://arxiv.org/abs/2506.00413>.

Jimenez, C. E., Yang, J., Wettig, A., Yao, S., Pei, K., Press, O., and Narasimhan, K. Swe-bench: Can language models resolve real-world github issues?, 2024. URL <https://arxiv.org/abs/2310.06770>.

Kang, W., Galim, K., Oh, S., Lee, M., Zeng, Y., Zhang, S., Hooper, C., Hu, Y., Koo, H. I., Cho, N. I., et al. Parallel-bench: Understanding the trade-offs of parallel decoding in diffusion llms. *arXiv preprint arXiv:2510.04767*, 2025.

Kim, J., Kim, S., Lee, T., Pan, D. Z., Kim, H., Kakade, S., and Chen, S. Fine-tuning masked diffusion for provable self-correction. *arXiv preprint arXiv:2510.01384*, 2025.

Kitanidis, E. and Hunter, C. J. pydra: Probing code representations with synthetic clones and bugs. In *NeurIPS 2025 Fourth Workshop on Deep Learning for Code*, 2025. URL <https://openreview.net/forum?id=SVVdrngi18>.

Labs, I., Khanna, S., Kharbanda, S., Li, S., Varma, H., Wang, E., Birnbaum, S., Luo, Z., Miraoui, Y., Palrecha, A., Ermon, S., Grover, A., and Kuleshov, V. Mercury: Ultra-fast language models based on diffusion, 2025. URL <https://arxiv.org/abs/2506.17298>.

Lee, S., Kim, S., Kim, S., Park, J., and Park, D. Effective test-time scaling of discrete diffusion through iterative refinement. *arXiv preprint arXiv:2511.05562*, 2025a.

Lee, Y.-J., Kim, S., Lee, B.-K., Moon, M., Hwang, Y., Kim, J. M., Neubig, G., Welleck, S., and Choi, H.-J. Refinebench: Evaluating refinement capability of language models via checklists, 2025b. URL <https://arxiv.org/abs/2511.22173>.

Li, X. L., Thickstun, J., Gulrajani, I., Liang, P., and Hashimoto, T. Diffusion-LM improves controllable text generation. In Oh, A. H., Agarwal, A., Belgrave, D., and Cho, K. (eds.), *Advances in Neural Information Processing Systems*, 2022. URL <https://openreview.net/forum?id=3s9IrEsjLyk>.

Liang, Y., Wang, Z., Chen, H., Sun, X., Wu, J., Yu, X., Liu, J., Barsoum, E., Liu, Z., and Jha, N. K. Cd4lm: Consistency distillation and adaptive decoding for diffusion language models, 2026. URL <https://arxiv.org/abs/2601.02236>.

Liu, A., He, M., Zeng, S., Zhang, S., Zhang, L., Wu, C., Jia, W., Liu, Y., Zhou, X., and Zhou, J. Wedlm: Reconciling diffusion language models with standard causal attention for fast inference, 2025a. URL <https://arxiv.org/abs/2512.22737>.

Liu, J., Xia, C. S., Wang, Y., and ZHANG, L. Is your code generated by chatGPT really correct? rigorous evaluation of large language models for code generation. In *Thirty-seventh Conference on Neural Information Processing Systems*, 2023. URL <https://openreview.net/forum?id=1qvx610Cu7>.

Liu, J., Dong, X., Ye, Z., Mehta, R., Fu, Y., Singh, V., Kautz, J., Zhang, C., and Molchanov, P. Tidar: Think in diffusion, talk in autoregression, 2025b. URL <https://arxiv.org/abs/2511.08923>.

Ni, J., Liu, Q., Du, C., Dou, L., Yan, H., Wang, Z., Pang, T., and Shieh, M. Q. Training optimal large diffusion language models, 2025. URL <https://arxiv.org/abs/2510.03280>.

Nie, S., Zhu, F., You, Z., Zhang, X., Ou, J., Hu, J., Zhou, J., Lin, Y., Wen, J.-R., and Li, C. Large language diffusion models, 2025. URL <https://arxiv.org/abs/2502.09992>.

NVIDIA, :, Basant, A., Khairnar, A., Paithankar, A., Khattar, A., Renduchintala, A., Malte, A., Bercovich, A., Hazare, A., Rico, A., Ficek, A., Kondratenko, A., Shaposhnikov, A., Bukharin, A., Taghibakhshi, A., Barton, A., Maha-baleshwarkar, A. S., Shen, A., Tao, A., Guan, A., Shors, A., Mandarwal, A., Mehta, A., Venkatesan, A., Sharabiani, A., Aithal, A., Poojary, A., Dattagupta, A., Bud-dharaju, B., Zhu, B., Simkin, B., Kartal, B., Rouhani, B. D., Chen, B., Ginsburg, B., Norick, B., Yu, B., Catan-zaro, B., Wang, C., Truong, C., Mungekar, C., Patel, C., Alexiuk, C., Munley, C., Parisien, C., Su, D., Afrimi, D., Korzekwa, D., Rohrer, D., Gitman, D., Mosallanezhad, D., Narayanan, D., Rekesh, D., Yared, D., Pykhtar, D., Ahn, D., Riach, D., Long, E., Ning, E., Chung, E., Galinkin, E., Bakhturina, E., Prasad, G., Shen, G., Qian, H., Elisha, H., Sharma, H., Ross, H., Ngo, H., Sahota, H., Wang, H., Shin, H. C., Huang, H., Cunningham, I., Gitman, I., Moshkov, I., Jung, J., Kautz, J., Scowcroft, J. P., Casper, J., Zhang, J., Zeng, J., Zhang, J., Xue, J., Huang, J., Conway, J., Kamalu, J., Cohen, J., Jennings, J., Vialard, J. V., Yi, J., Parmar, J., Briski, K., Cheung, K., Luna, K., Wyss, K., Santhanam, K., Kong, K., Pawelec, K., Anik, K., Li, K., Ahmadian, K., McAfee, L., Sleiman, L., Der-czynski, L., Vega, L., de Melo, M. R., Sreedhar, M. N., Chochowski, M., Cai, M., Kliegl, M., Stepniewska-Dziubinska, M., Novikov, M., Samadi, M., Price, M., Boubdir, M., Boone, M., Evans, M., Bien, M., Zawal-ski, M., Martinez, M., Chrzanowski, M., Shoeybi, M., Patwary, M., Dhameja, N., Assaf, N., Habibi, N., Bhatia, N., Pope, N., Tajbakhsh, N., Juluru, N. K., Rybakov, O., Hrinchuk, O., Kuchaiev, O., Olabiyi, O., Ribalta, P., Subramanian, P., Chadha, P., Molchanov, P., Dykas, P., Jin, P., Bialecki, P., Januszewski, P., Thalasta, P., Gaikwad, P., Varshney, P., Gundecha, P., Tredak, P., Mahabadi, R. K., Patel, R., El-Yaniv, R., Rajan, R., Cheruvu, R., Shah-bazyan, R., Borkar, R., Gala, R., Waleffe, R., Zhang, R., Hewett, R. J., Prenger, R., Jain, S., Kriman, S., Satheesh, S., Kaji, S., Yurick, S., Muralidharan, S., Narenthiran, S., Bak, S., Sameni, S., Han, S., Ramasamy, S., Ghosh, S., Sreenivas, S. T., Thomas, S., Diao, S., Gopal, S., Prab-humoye, S., Toshniwal, S., Ding, S., Singh, S., Jain, S., Majumdar, S., Singhal, S., Alborghetti, S., Akter, S. N., Kong, T., Moon, T., Hliwiak, T., Asida, T., Wang, T., Konuk, T., Vashishth, T., Poon, T., Karpas, U., Noroozi, V., Srinivasan, V., Korthikanti, V., Fugro, V., Kalluru, V., Kurin, V., Lavrukhin, V., Ahmad, W. U., Du, W., Byeon, W., Lu, X., Dong, X., Karnati, Y., Choi, Y., Zhang, Y., Lin, Y., Fu, Y., Suhara, Y., Dong, Z., Li, Z., Zhu, Z., and Chen, Z. Nvidia nemotron nano 2: An accurate and efficient hybrid mamba-transformer reasoning model, 2025. URL <https://arxiv.org/abs/2508.14444>.

Opu, M. N. I., Wang, S., and Chowdhury, S. Llm-based detection of tangled code changes for higher-quality method-level bug datasets, 2025. URL <https://arxiv.org/abs/2505.08263>.

Peng, F. Z., Bezemek, Z., Patel, S., Rector-Brooks, J., Yao, S., Tong, A., and Chatterjee, P. Path planning for masked diffusion models with applications to biological sequence generation. In *ICLR 2025 Workshop on Deep Generative Model in Machine Learning: Theory, Principle and Efficacy*, 2025a. URL <https://openreview.net/forum?id=fFuVPKpSt0>.

Peng, F. Z., Zhang, S., Tong, A., and Open-dLLM Contributors. Open-dLLM: Open diffusion large language models, 2025b. URL <https://github.com/pengzhangzhi/Open-dLLM>.

Reid, M., Hellendoorn, V. J., and Neubig, G. DiffusER: Diffusion via edit-based reconstruction. In *The Eleventh International Conference on Learning Representations*, 2023. URL <https://openreview.net/forum?id=nG9RF9z1yy3>.

Sahoo, S. S., Arriola, M., Gokaslan, A., Marroquin, E. M., Rush, A. M., Schiff, Y., Chiu, J. T., and Kuleshov, V. Simple and effective masked diffusion language models. In *The Thirty-eighth Annual Conference on Neural Information Processing Systems*, 2024. URL <https://openreview.net/forum?id=L4uaAR4ArM>.

Schiff, Y., Sahoo, S. S., Phung, H., Wang, G., Boshar, S., Dalla-torre, H., de Almeida, B. P., Rush, A. M., PIER-ROT, T., and Kuleshov, V. Simple guidance mechanisms for discrete diffusion models. In *The Thirteenth International Conference on Learning Representations*, 2025. URL <https://openreview.net/forum?id=i5MrJ6g5G1>.

Song, Y., Zhang, Z., Luo, C., Gao, P., Xia, F., Luo, H., Li, Z., Yang, Y., Yu, H., Qu, X., Fu, Y., Su, J., Zhang, G., Huang, W., Wang, M., Yan, L., Jia, X., Liu, J., Ma, W.-Y., Zhang, Y.-Q., Wu, Y., and Zhou, H. Seed diffusion: A large-scale diffusion language model with high-speed

inference, 2025. URL <https://arxiv.org/abs/2508.02193>.

Tang, Z., Li, Z., Xiao, Z., Ding, T., Sun, R., Wang, B., Liu, D., Huang, F., Liu, T., Yu, B., and Lin, J. Realcritic: Towards effectiveness-driven evaluation of language model critiques, 2025. URL <https://arxiv.org/abs/2501.14492>.

von Rütte, D., Fluri, J., Ding, Y., Orvieto, A., Schölkopf, B., and Hofmann, T. Generalized interpolating discrete diffusion. In *Forty-second International Conference on Machine Learning*, 2025. URL <https://openreview.net/forum?id=rvZv7sDPV9>.

Wang, G., Schiff, Y., Sahoo, S. S., and Kuleshov, V. Remasking discrete diffusion models with inference-time scaling. In *The Thirty-ninth Annual Conference on Neural Information Processing Systems*, 2025a. URL <https://openreview.net/forum?id=IJryQA0y0p>.

Wang, K., Jiang, Z., Feng, H., Zhao, W., Liu, L., Li, J., Lan, Z., and Lin, W. Creditdecoding: Accelerating parallel decoding in diffusion large language models with trace credits, 2025b. URL <https://arxiv.org/abs/2510.06133>.

Widyasari, R., Sim, S. Q., Lok, C., Qi, H., Phan, J., Tay, Q., Tan, C., Wee, F., Tan, J. E., Yieh, Y., Goh, B., Thung, F., Kang, H. J., Hoang, T., Lo, D., and Ouh, E. L. Bugsipy: a database of existing bugs in python programs to enable controlled testing and debugging studies. In *Proceedings of the 28th ACM Joint Meeting on European Software Engineering Conference and Symposium on the Foundations of Software Engineering*, ESEC/FSE 2020, pp. 1556–1560, New York, NY, USA, 2020. Association for Computing Machinery. ISBN 9781450370431. doi: 10.1145/3368089.3417943. URL <https://doi.org/10.1145/3368089.3417943>.

Wu, C., Zhang, H., Xue, S., Diao, S., Fu, Y., Liu, Z., Molchanov, P., Luo, P., Han, S., and Xie, E. Fast-dllm v2: Efficient block-diffusion llm, 2025a. URL <https://arxiv.org/abs/2509.26328>.

Wu, C., Zhang, H., Xue, S., Liu, Z., Diao, S., Zhu, L., Luo, P., Han, S., and Xie, E. Fast-dllm: Training-free acceleration of diffusion llm by enabling kv cache and parallel decoding, 2025b. URL <https://arxiv.org/abs/2505.22618>.

Wu, S. and Zhang, J. Free draft-and-verification: Toward lossless parallel decoding for diffusion large language models, 2025. URL <https://arxiv.org/abs/2510.00294>.

Yang, A., Li, A., Yang, B., Zhang, B., Hui, B., Zheng, B., Yu, B., Gao, C., Huang, C., Lv, C., Zheng, C., Liu, D., Zhou, F., Huang, F., Hu, F., Ge, H., Wei, H., Lin, H., Tang, J., Yang, J., Tu, J., Zhang, J., Yang, J., Yang, J., Zhou, J., Zhou, J., Lin, J., Dang, K., Bao, K., Yang, K., Yu, L., Deng, L., Li, M., Xue, M., Li, M., Zhang, P., Wang, P., Zhu, Q., Men, R., Gao, R., Liu, S., Luo, S., Li, T., Tang, T., Yin, W., Ren, X., Wang, X., Zhang, X., Ren, X., Fan, Y., Su, Y., Zhang, Y., Zhang, Y., Wan, Y., Liu, Y., Wang, Z., Cui, Z., Zhang, Z., Zhou, Z., and Qiu, Z. Qwen3 technical report, 2025. URL <https://arxiv.org/abs/2505.09388>.

Ye, J., Xie, Z., Zheng, L., Gao, J., Wu, Z., Jiang, X., Li, Z., and Kong, L. Dream 7b: Diffusion large language models, 2025. URL <https://arxiv.org/abs/2508.15487>.

Zhang, A., Sivakumar, A., Tang, C.-W., and Thomas, C. Flexible-length text infilling for discrete diffusion models. In Christodoulopoulos, C., Chakraborty, T., Rose, C., and Peng, V. (eds.), *Proceedings of the 2025 Conference on Empirical Methods in Natural Language Processing*, pp. 31332–31347, Suzhou, China, November 2025. Association for Computational Linguistics. ISBN 979-8-89176-332-6. doi: 10.18653/v1/2025.emnlp-main.1597. URL <https://aclanthology.org/2025.emnlp-main.1597>.

Zhu, F., You, Z., Xing, Y., Huang, Z., Liu, L., Zhuang, Y., Lu, G., Wang, K., Wang, X., Wei, L., Guo, H., Hu, J., Ye, W., Chen, T., Li, C., Tang, C., Feng, H., Hu, J., Zhou, J., Zhang, X., Lan, Z., Zhao, J., Zheng, D., Li, C., Li, J., and Wen, J.-R. Llada-moe: A sparse moe diffusion language model, 2025. URL <https://arxiv.org/abs/2509.24389>.

## Contents of the Appendix

The appendix includes the following contents:

- Sec. A discusses limitations of the proposed benchmark and training formulation.
- Sec. B discusses related work.
- Sec. D presents a self-revision analysis under minimal corruption.
- Sec. C provides aggregated Pass@1 Results on CRB Benchmark.
- Sec. E provides implementation details of Section. 7
- Sec. F provides a controlled from-scratch analysis of corrective behavior on Sudoku.
- Sec. G presents the remask-based iterative refinement procedure.

### A. Limitations

Our goal is to isolate localized corrective behavior under masked diffusion and remask-based refinement, which aligns with the formulation commonly adopted by current foundation-model-style DLMs (Nie et al., 2025; Ye et al., 2025; Peng et al., 2025b). Accordingly, our study focuses on fixed-length correction settings, and the proposed Code Revision Benchmark (CRB) is designed to evaluate localized token replacement under exact token alignment. As a result, CRB does not directly support the evaluation of models that perform insertion or deletion operations, or more general variable-length editing, as explored in recent discrete diffusion formulations (Havasi et al., 2025; Chao et al., 2025; Zhang et al., 2025; Reid et al., 2023). Extending executable revision benchmarks to support variable-length editing and broader editing paradigms remains an interesting direction for future work.

### B. Related Work

#### B.1. Development of DLMs

The development of diffusion-based language modeling begins with continuous-space approaches such as DiffusionLM (Li et al., 2022), which apply Gaussian noise in continuous space over token embeddings but remain misaligned with the discrete nature of textual data. The introduction of D3PM (Austin et al., 2021a) establishes a unified framework for discrete-state diffusion through flexible transition kernels, encompassing uniform, absorbing, and structured corruption processes. Exploration of uniform-noise discrete diffusion, exemplified by Schiff et al. (2025), demonstrates limited suitability for natural language due to excessive semantic destruction. Absorbing-noise diffusion subsequently emerges as a more stable alternative for text. DiffusionBERT (He et al., 2023) shows that using a single absorbing token (e.g., [MASK]) significantly improves training dynamics and sample quality. Building on these developments, the masked diffusion language model (MDLM) formulation (Sahoo et al., 2024) interprets masked diffusion as a variational objective composed of weighted masked language modeling (MLM)-style reconstruction terms and achieves strong performance among discrete DLMs. Systematic scaling studies (Ni et al., 2025; Nie et al., 2025) further confirm that MDLM can outperform AR models when scaling up.

#### B.2. Self-correction in DLMs.

Recent work has shown that DLMs may accumulate errors during parallel decoding. Kang et al. (2025) and Chen et al. (2025) demonstrate that parallel denoising steps can introduce or amplify token-level inconsistencies, highlighting the need for mechanisms that explicitly identify and correct decoding errors. A number of subsequent approaches address this issue by incorporating remasking strategies or auxiliary guidance during inference. Peng et al. (2025a) propose a remask-based decoding procedure that relies on an external planner to select tokens for resampling, while Wang et al. (2025a) introduce remasking discrete diffusion models that guide inference-time remasking using token-level confidence to improve generation quality without additional training. Similarly, Lee et al. (2025a) employ an auxiliary scoring model to assess intermediate predictions and determine whether remasking is necessary. Kim et al. (2025) further integrate remasking decisions into the model itself by introducing an internal prediction head that estimates, for each token, the probability that it should be

remasked, enabling model-internal correction without external supervision. Most relevant to our work, von Rütte et al. (2025) propose the Generalized Interpolating Discrete Diffusion framework, which combines absorbing and uniform noise to generalize discrete diffusion and improve generation quality. Despite similarities in noise design, this framework differs fundamentally in its sampling mechanism: it performs holistic diffusion updates in which all token positions may change across denoising steps. In contrast, our approach follows the masked diffusion paradigm, in which decoding explicitly restricts updates to masked or remasked positions.

### B.3. Efficient Decoding in DLMs

The inference speed of diffusion language models (DLMs) is fundamentally limited by the trade-off between parallel decoding efficiency and output quality. A growing body of work has investigated parallel decoding strategies to mitigate this issue.

One line of research adapts speculative decoding from autoregressive models to the diffusion setting, enabling simultaneous decoding of multiple tokens. Self Speculative Decoding introduces a speculative decoding framework tailored for DLMs (Gao et al., 2025). Reformulating the classic draft–verify paradigm, Wu & Zhang (2025) propose a self-verifiable decoding mechanism that enables lossless parallel decoding. Related approaches incorporate auxiliary verification signals: Israel et al. (2025) employ a smaller verification model to dynamically adjust the number of decoded tokens based on error estimates.

Beyond explicit verification, other methods improve efficiency through token-level commitment strategies. Liang et al. (2026) propose Confidence-Adaptive Decoding, which accelerates inference by committing high-confidence tokens early, while Wang et al. (2025b) introduce CreditDecoding, leveraging historical logits to estimate token convergence and guide more efficient parallelization.

Another line of work addresses the lack of key–value (KV) caching in standard DLMs, which stems from their use of bidirectional attention, preventing reuse of cached keys and values across refinement steps and thereby limiting inference efficiency compared to autoregressive models. Block Diffusion introduces block-wise generation to enable KV cache reuse across decoding steps (Arriola et al., 2025). Fast-dLLM proposes a training-free block-wise parallel decoding strategy with KV caching (Wu et al., 2025b), and Fast-dLLM v2 further extends this approach with hierarchical caching mechanisms (Wu et al., 2025a). Causal parallel decoding via Jacobi Forcing designs a rejection–recycling and multi-block decoding algorithm to improve inference efficiency (Hu et al., 2025). TiDAR integrates speculative decoding with KV cache reuse by employing a diffusion model as a parallel drafter (Liu et al., 2025b), while WeDLM proposes a prefix-cache-compatible streaming parallel decoding strategy using causal masking and a dynamic sliding window to alleviate the bottleneck of block decoding (Liu et al., 2025a).

### B.4. Self-Correction and Refinement in Large Language Models

A number of prior studies on large language models have explored concepts related to correction and refinement across general datasets and multiple domains, often under the formulation of self-correction, critique, or iterative improvement. Huang et al. (2024) study models’ ability to self-correct on reasoning-oriented benchmarks, focusing on improving final answers through iterative reasoning. RealCritic (Tang et al., 2025) proposes a critique-and-correction framework that explicitly models how the quality of critiques affects downstream solution refinement, while RefineBench (Lee et al., 2025b) allows models to autonomously decide whether refinement is necessary and to generate self-feedback before revision. In task-specific settings, particularly for code, several benchmarks have been proposed to evaluate code editing and repair capabilities under more realistic scenarios. Tangled Code Changes (Opu et al., 2025), BugsInPy (Widyasari et al., 2020), and Pydra (Kitanidis & Hunter, 2025) construct benchmarks based on real or synthetic bugs to evaluate code correction capabilities. More recent benchmarks such as CodeEditorBench (Guo et al., 2025b), SWE-Bench (Jimenez et al., 2024), and EditBench (Chi et al., 2025) further study code editing in realistic development settings, often requiring models to perform multi-line, instruction-driven, or repository-level modifications.

While these benchmarks demonstrate that language models can revise and improve their outputs under various correction paradigms, they predominantly treat correction as a task-level or procedural process that generates revised solutions from scratch or through external critique loops. In particular, refinement in these settings is typically not performed *in place* on a complete input, but instead relies on regeneration, multi-stage prompting, or auxiliary feedback mechanisms. In contrast, our Code Revision Benchmark (CRB) isolates *in-place refinement* by applying localized corruptions to a complete input and evaluating whether a model can identify and correct erroneous tokens while preserving correct context.

Table 4. Pass@1 on refinement-based code correction across standard coding benchmarks for MDLM, CDLM, and the base model. Results are aggregated over all error types and corruption levels using 4 refinement steps with a confidence threshold of 0.9. CDLM consistently outperforms MDLM and the base model across datasets.

Dataset	MDLM	CDLM	Base
HumanEval	0.157	0.257	0.168
HumanEval+	0.182	0.242	0.196
MBPP	0.114	0.175	0.114
MBPP+	0.137	0.226	0.120
<b>Average</b>	<b>0.148</b>	<b>0.225</b>	<b>0.150</b>

Table 5. Self-revision under minimal corruption on HumanEval. For each model, we first generate programs and retain only those that pass all tests. A single type-preserving token corruption ( $n_{\text{replace}} = 1$ ) is then applied to each correct program, and the model is evaluated on its ability to revise the corrupted program back to a passing solution using iterative refinement. Reported values correspond to Pass@1 after different numbers of refinement steps.

Model	T=1	T=2	T=3	T=4
LLaDA-8B-Base	0.550	0.571	0.577	0.580
Dream-7B-Base	0.528	0.548	0.402	0.427
Open-dCoder-0.5B	0.203	0.342	0.344	0.336

## C. Aggregated Pass@1 Results on CRB

Table 4 reports aggregated Pass@1 for refinement-based code correction on standard benchmarks (HumanEval/HumanEval+/MBPP/MBPP+), using 4 refinement steps with a confidence threshold of 0.9, comparing MDLM, CDLM, and the base model.

## D. Self-revision under minimal corruption

The Code Revision Benchmark (CRB) constructs revision instances by introducing controlled corruptions to canonical programs. While this design isolates error localization and correction behavior, there is a risk that a model may fail to revise a corrupted program simply because the input falls outside the distribution of code it typically generates. In such cases, poor revision performance could reflect distributional mismatch rather than a genuine inability to detect and correct errors.

To disentangle these factors, we design a *self-revision under minimal corruption* setting, in which each model is evaluated exclusively on programs that it has already demonstrated the ability to generate correctly. By introducing only a minimal, localized perturbation to model-generated solutions, this setting ensures that revision failures cannot be attributed to unfamiliar inputs, and instead directly probe the model’s capacity for targeted error detection and correction.

**Setup.** For each model, we first identify a set of programs that the model can generate correctly under standard decoding. Starting from these correct model-generated programs, we introduce a single type-preserving token corruption ( $n_{\text{replace}} = 1$ ) using the CRB corruption pipeline. Restricting to a single-token modification ensures that the corrupted program remains extremely close to the model’s own generation distribution, differing from a correct solution only through a minimal and localized perturbation. This design isolates the model’s ability to recognize and revise a small error, rather than its capacity to handle large semantic changes or distributional shifts.

We then apply iterative refinement to the corrupted program and evaluate whether the model can revise it back to a correct solution. Performance is measured using Pass@1 after varying numbers of refinement steps, ranging from 1 to 4.

**Results and Discussion.** Table 5 evaluates self-revision performance under a single-token corruption setting. Even when starting from programs that each model has itself generated and verified as correct, all evaluated DLMs achieve low Pass@1 after revision. Increasing the number of refinement steps from 1 to 4 yields only marginal and non-monotonic improvements, indicating that additional iterations do not reliably enhance correction performance. These failures persist despite the minimal and localized nature of the corruption and the fact that the original programs lie squarely within each model’s own generation distribution. Although the models are capable of generating correct programs, they often fail to identify and repair even a single incorrect token once it is introduced.

Table 6. Pass@1 and Pass@10 on MBPP and MBPP+ under two decoding variants. *Vanilla* recomputes token confidence at every refinement step, while *ReMDM* fixes each token’s confidence at its first unmasking step (Wang et al., 2025a). The **Avg** column averages MBPP and MBPP+. Boldface highlights CDLM improvements over the absorbing-only MDLM baseline under the same decoding setting.

Method	MBPP		MBPP+		Avg	
	Pass@1	Pass@10	Pass@1	Pass@10	Pass@1	Pass@10
MDLM (Vanilla)	0.106	0.312	0.177	0.449	0.141	0.381
CDLM (Vanilla)	<b>0.131</b>	<b>0.352</b>	<b>0.207</b>	<b>0.472</b>	<b>0.169</b>	<b>0.412</b>
Base (Vanilla)	0.157	0.350	0.231	0.502	0.194	0.426
MDLM (ReMDM)	0.108	0.328	0.170	0.444	0.139	0.386
CDLM (ReMDM)	<b>0.141</b>	<b>0.350</b>	<b>0.211</b>	<b>0.476</b>	<b>0.176</b>	<b>0.413</b>
Base (ReMDM)	0.160	0.366	0.232	0.485	0.196	0.425

## E. Implementation Details of CDLM Training

This appendix provides implementation details for the training setups used in our experiments, corresponding to the code generation and ParallelBench evaluations reported in the main paper.

### E.1. Code Generation Fine-Tuning

For the code generation experiments, we fine-tune the OPEN-DCODER-0.5B checkpoint (Peng et al., 2025b) for 2000 optimization steps on the Nemotron coding corpus (NVIDIA et al., 2025). The Nemotron corpus consists of high-quality code samples spanning multiple programming languages and problem domains.

Throughout the code generation section, we compare three models: (i) the pretrained base model without additional fine-tuning, (ii) a model fine-tuned using the absorbing-only objective (MDLM), and (iii) the mixture-trained CDLM-0.5B. The training configurations for (ii) and (iii) are identical except for the choice of training objective. In particular, both models share the same optimizer, learning rate schedule, batch size, noise schedule, and remasking configuration, ensuring that observed differences are attributable solely to the training objective.

**MBPP Results.** In the main paper, we focus on HumanEval and HumanEval+ for compact presentation, and report MBPP/MBPP+ in this appendix. Table 6 summarizes Pass@1 and Pass@10 on MBPP and MBPP+, along with an average over the two benchmarks. Across both vanilla confidence-based decoding and ReMDM decoding, CDLM consistently outperforms the absorbing-only MDLM baseline on MBPP and MBPP+. However, CDLM is slightly below the pretrained base model on these benchmarks. We attribute this to dataset-specific distribution differences: the base checkpoint may align better with MBPP-style problems, whereas fine-tuning on Nemotron introduces a mild shift that affects MBPP/MBPP+ more than HumanEval-style evaluations. Importantly, the consistent improvements of CDLM over MDLM indicate that the mixture objective remains beneficial, and the gap to the base model is more likely driven by distribution mismatch rather than a systematic limitation of CDLM.

### E.2. ParallelBench Fine-Tuning

For the ParallelBench experiments, we fine-tune LLADA-2.0-MINI (16B) (Bie et al., 2025) on data generated from the ParallelBench benchmark (Kang et al., 2025). We construct a training set of 50,000 examples and fine-tune the model for 6 epochs using block diffusion (Arriola et al., 2025).

During training, the mask ratio is sampled uniformly from  $[0, 1]$  for each example. We adopt block diffusion with a block size of 32, consistent with the decoding configuration used at evaluation time. Since ParallelBench tasks involve short outputs, the maximum generation length is capped at 64 tokens.

At inference time, we use confidence-based decoding with two modes, fixed and remask. In the fixed mode, tokens are generated without further remasking. In the remask mode, previously unmasked tokens with low confidence are remasked and regenerated in subsequent steps. We set the confidence threshold to 0.6 to increase parallelism during decoding.

**ParallelBench Data Format and Tasks.** ParallelBench consists of structured transformation tasks designed to evaluate parallel decoding under high output uncertainty. Each example includes a natural language instruction and a short input

sequence, and the model must generate an output that satisfies the specified transformation. Many tasks admit multiple valid outputs, making exact prediction unlikely and iterative refinement essential.

Below we illustrate three representative tasks used in our experiments with concrete examples.

**Shuffle** requires the model to randomly permute the input sequence while ensuring that the output differs from the original order. *Instruction*: Randomly shuffle the waiting line. *Input*: `["Paul Payne", "Robert Riley", "Peter Stone"]`. *Output*: Any permutation different from the input (e.g., `["Robert Riley", "Peter Stone", "Paul Payne"]`).

**Replace Index** requires replacing the element at a specified position with a given value. *Instruction*: Replace the person at position 0 with "Henry Warren". *Input*: `["Patrick Morgan", "Eric King", "Joe Reed"]`. *Output*: `["Henry Warren", "Eric King", "Joe Reed"]`.

**Replace Random** requires replacing one randomly chosen element in the sequence with a given value. *Instruction*: Replace one random person with "Juan Torres". *Input*: `["David Owens", "Kelly Payne", "Aaron Freeman"]`. *Output*: Any list where exactly one name is replaced by "Juan Torres".

Some of these tasks naturally induce high output entropy, particularly in the *Shuffle* and *Replace Random* settings. As a result, errors arise primarily from parallel decoding rather than externally injected noise, making ParallelBench well suited for evaluating correction-aware training under high-uncertainty generation.

## F. Sudoku: A Controlled From-Scratch Proxy for Pretraining

To further validate the proposed training principle in a fully controlled setting, we conduct additional experiments on Sudoku and report the results. Sudoku is a compact symbolic domain in which the full data distribution is observable and correctness is deterministically verifiable. This environment allows us to isolate learning dynamics induced by the noising process and training objective, without interference from prior knowledge or data ambiguity. It therefore provides a clean testbed for examining whether the proposed post-training objective induces error-aware confidence and iterative corrective behavior.

Our Sudoku CDLM uses a Diffusion Transformer (DiT) architecture with approximately 37M parameters (12 layers, hidden size 512, 8 attention heads, MLP ratio 4, dropout 0.1), following the experimental setup of [Kim et al. \(2025\)](#). Each puzzle is represented as an 81-token sequence over a vocabulary of size 10 (a MASK token and digits 1–9). Training uses 36,000 puzzles, batch size 64, 200,000 optimization steps, learning rate  $1 \times 10^{-4}$ , weight decay 0.01, and a dynamically sampled masking ratio in  $[0.2, 0.9]$ .

This controlled from-scratch environment allows us to isolate and evaluate two core aspects of corrective behavior: (i) whether training with the mixture objective induces error-awareness, namely the ability to assign lower confidence to corrupted tokens than to clean ones; and (ii) whether improved error localization translates into more effective iterative, in-place correction. In addition, we assess whether the mixture training objective improves standard absorbing-noise reconstruction, corresponding to pure denoising-based generation without uniform corruptions.

### F.1. Uniform Noise Corruption: Error-Token Localization

We begin by evaluating whether the mixture objective induces error-aware confidence calibration under uniform noise corruption. Using a single forward pass without iterative refinement, a fraction of positions is corrupted by replacing the

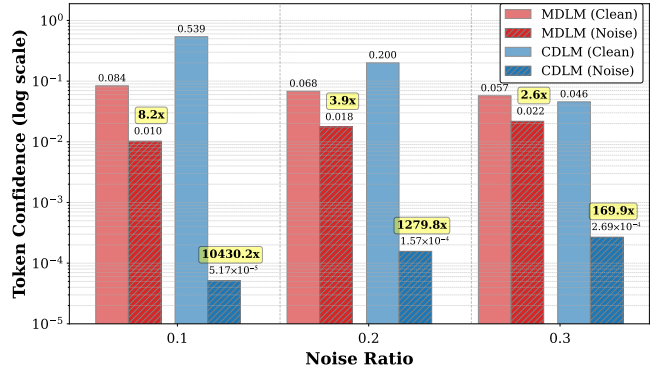


*Figure 8.* Confidence on clean and noisy digits under uniform corruption (log scale). We report clean–noise confidence ratios (yellow annotations) rather than absolute confidence gaps, since confidence values span multiple orders of magnitude in this setting. CDLM exhibits substantially larger clean–noise separation than MDLM across noise ratios, indicating significantly improved error localization compared with the absorbing-only objective.

original digit with a uniformly sampled incorrect digit. We then measure the model’s confidence on clean versus corrupted positions. This setting isolates the effect of uniform-noise supervision on token-level confidence, independent of any iterative sampling dynamics.

Figure 8 reports confidence statistics across noise ratios of 0.1, 0.2, and 0.3. Models trained with the absorbing-only objective exhibit only weak separation between clean and corrupted digits. For example, at a noise ratio of 0.1, the ratio between mean confidence on clean digits and noisy digits is approximately  $8.2\times$ . In contrast, models trained with the mixture objective exhibit substantially stronger separation: the clean–noise confidence ratio exceeds  $10,000\times$  at noise ratio 0.1 and remains above  $160\times$  even at noise ratio 0.3.

These results show that mixture objective training induces strong error-awareness in the model’s confidence estimates. Corrupted digits are consistently assigned low confidence while clean digits retain high confidence, providing a reliable signal for error localization. This calibrated confidence forms a critical prerequisite for effective remask-based iterative correction, which we evaluate next.

## F.2. Iterative Correction under Uniform Noise

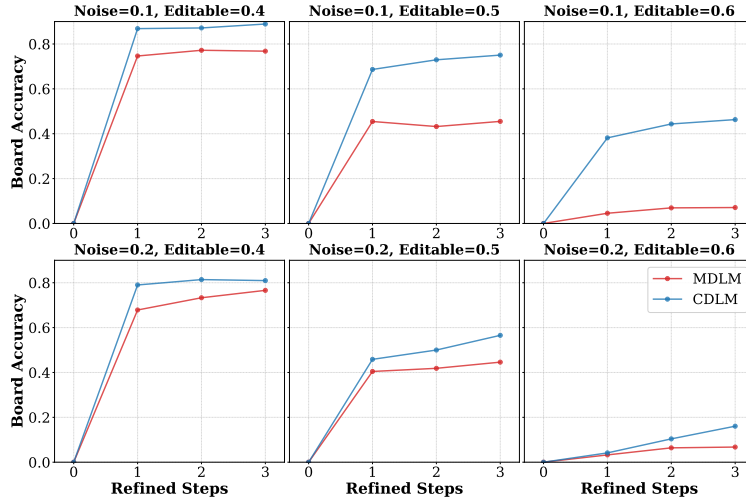


Figure 9. Sudoku board accuracy under uniform corruption with iterative diffusion sampling. Each subplot shows accuracy as a function of refinement steps for a specific combination of noise ratio and editable ratio. Across all difficulty settings, CDLM consistently achieves higher accuracy than MDLM.

We next study whether the improved error localization learned by CDLM translates into more effective iterative correction. Starting from grids corrupted by uniform noise, we define an editable region that always includes all noisy positions and may additionally include clean positions according to a specified editable ratio. Refinement is performed by iteratively remasking and resampling tokens within the editable region, while treating all other cells as fixed conditioning context. The full remask-based refinement procedure, including confidence computation and update rules, is detailed in Appendix G.2 (Algorithm 2). We vary the noise ratio, the editable ratio, and the number of refinement steps, and evaluate board accuracy after the final refinement step.

Figure 9 summarizes results for two noise ratios (0.1 and 0.2), three editable ratios (0.4, 0.5, 0.6), and up to three refinement steps. Across all settings, CDLM consistently achieves higher board accuracy than MDLM. This advantage is already visible after a single refinement step and often increases with additional steps. These results suggest that the improved confidence calibration learned by CDLM facilitates not only better error localization, but also more effective guided, in-place refinement under uniform corruption.

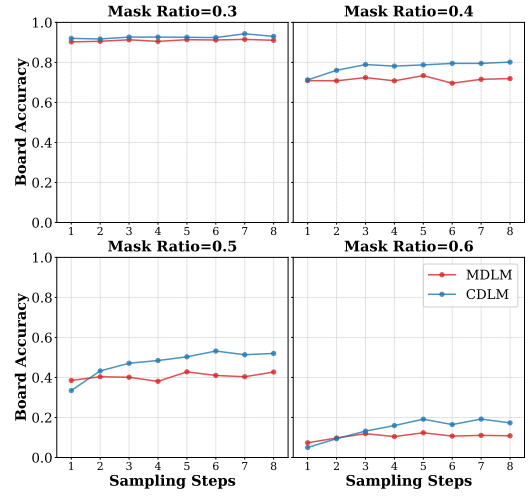


Figure 10. Pure completion performance under absorbing-mask corruption. Each subplot shows board accuracy as a function of sampling steps for a fixed mask ratio. Across all mask settings, CDLM matches or exceeds MDLM performance, indicating that the mixture objective does not introduce a tradeoff in reconstruction ability.

**Algorithm 1** Confidence-Based Iterative Refinement with Remasking

---

**Input:** Initial sequence  $\mathbf{z}^{(0)} \in (\mathcal{V} \cup \{\langle \text{mask} \rangle\})^n$ ;  
 Denoising model  $p_\theta(\cdot | \cdot)$ ;  
 Confidence threshold  $\tau \in (0, 1)$ ;  
 Number of refinement steps  $T$   
**Output:** Refined sequence  $\mathbf{z}^{(T)}$

**for**  $t = 0, 1, \dots, T - 1$  **do**

// Parallel denoising prediction

Compute token distributions  $p_\theta(\cdot | \mathbf{z}^{(t)})$  for all positions   Compute confidences  $c_i^{(t)} = \max_{v \in \mathcal{V}} p_\theta(v | \mathbf{z}^{(t)})$  for all  $i$

Compute predictions

$$\hat{x}_i^{(t)} = \begin{cases} \arg \max_{v \in \mathcal{V}} p_\theta(v | \mathbf{z}^{(t)}), & z_i^{(t)} = \langle \text{mask} \rangle \\ z_i^{(t)}, & \text{otherwise} \end{cases} \quad \text{for all } i$$

// Identify low-confidence positions

$$r^{(t)} \leftarrow \{i \in \{1, \dots, n\} \mid c_i^{(t)} < \tau\}$$

// Remasking and update

**foreach**  $i = 1, \dots, n$  **do**

$z_i^{(t+1)} \leftarrow \begin{cases} \langle \text{mask} \rangle, & i \in r^{(t)} \\ \hat{x}_i^{(t)}, & \text{otherwise} \end{cases}$

**return**  $\mathbf{z}^{(T)}$

---

### F.3. Pure Completion under Masked Denoising

We finally evaluate the effect of the mixture objective in a pure completion setting. Unlike the refinement experiments, this setup does not involve uniformly corrupted digits. Instead, a fraction of positions is replaced with a mask token, and the model performs multi-step denoising to produce a complete Sudoku grid using confidence-guided remask-based decoding. This setting corresponds to standard masked denoising and serves to assess whether training for corrective behavior also benefits pure denoising-based generation.

Figure 10 reports board accuracy across mask ratios from 0.3 to 0.6 using confidence-guided decoding with a threshold of 0.7. Models trained with the mixture objective consistently match or outperform those trained with the absorbing-only objective across all mask levels. The improvement is particularly pronounced at higher mask ratios, where confidence-guided refinement enables the model to identify and revise low-confidence digits during the denoising process. These results demonstrate that incorporating uniform-noise supervision not only preserves pure completion performance, but can also improve robustness in challenging masked reconstruction regimes.

## G. Remask-Based Iterative Refinement Algorithm

### G.1. Remask-Based Iterative Refinement Procedure in DLMs

Algorithm 1 summarizes the confidence-based iterative refinement procedure used throughout our experiments. At each step, low-confidence tokens are explicitly remasked and resampled, while all other tokens are treated as fixed conditioning context. Unlike GIDD (von Rütte et al., 2025), which performs holistic diffusion updates over all token positions and does not employ an explicit remasking mechanism, this procedure explicitly restricts updates to masked or remasked positions, enabling localized, in-place refinement.

### G.2. Remask-Based Iterative Refinement for Sudoku under Uniform Noise

We consider Sudoku boards represented as sequences of length 81, where each token takes values from a discrete vocabulary  $\mathcal{V} = \{\langle \text{mask} \rangle, 1, \dots, 9\}$ . Given an initial grid corrupted by uniform replacement noise, we define an *editable set* of token positions  $\mathcal{E} \subseteq \{1, \dots, 81\}$ . By construction,  $\mathcal{E}$  always contains all uniformly corrupted (noisy) positions, and may additionally include a subset of clean positions according to a specified editable ratio.

---

**Algorithm 2** Remask-Based Iterative Refinement with Editable Tokens (Sudoku)

---

**Input:** Initial sequence  $\mathbf{z}^{(0)} = (z_1^{(0)}, \dots, z_{81}^{(0)})$ ,  $z_i^{(0)} \in \mathcal{V} = \{\langle \text{mask} \rangle, 1, \dots, 9\}$ , corrupted by uniform replacement noise; Denoising model  $p_\theta(\cdot | \cdot)$ ; Editable token set  $\mathcal{E} \subseteq \{1, \dots, 81\}$  containing all noisy positions; Confidence threshold  $\tau$ ; Number of refinement steps  $T$ .

**Output:** Refined sequence  $\mathbf{z}^{(T)}$ .

**for**  $t = 0, 1, \dots, T - 1$  **do**

// Denoising prediction (token predictions and confidence)

**for**  $i = 1, 2, \dots, 81$  **do**

Compute  $p_\theta(\cdot | \mathbf{z}^{(t)})$  at position  $i$ ;

$\hat{x}_i^{(t)} \leftarrow \arg \max_{v \in \mathcal{V} \setminus \{\langle \text{mask} \rangle\}} p_\theta(v | \mathbf{z}^{(t)})$ ;

$c_i^{(t)} \leftarrow \max_{v \in \mathcal{V} \setminus \{\langle \text{mask} \rangle\}} p_\theta(v | \mathbf{z}^{(t)})$ .

// Identify remasking set (restricted to editable tokens)

$\mathcal{R}^{(t)} \leftarrow \{i \in \mathcal{E} : c_i^{(t)} < \tau\}$ ;

// Construct next iterate; non-editable tokens remain fixed

**for**  $i = 1, 2, \dots, 81$  **do**

**if**  $i \in \mathcal{R}^{(t)}$  **then**

$z_i^{(t+1)} \leftarrow \langle \text{mask} \rangle$ ;

**else**

**if**  $i \in \mathcal{E}$  **then**

$z_i^{(t+1)} \leftarrow \hat{x}_i^{(t)}$ ;

**else**

$z_i^{(t+1)} \leftarrow z_i^{(t)}$ ; ;

// Non-editable tokens remain unchanged

**return**  $\mathbf{z}^{(T)}$

---

**Notes.** The editable set  $\mathcal{E}$  is fixed throughout decoding and is constructed *a priori* for controlled evaluation. The remasking set  $\mathcal{R}^{(t)}$  is recomputed at every step based on token-level confidence, but is always restricted to  $\mathcal{E}$ . As a result, the procedure performs localized, in-place correction by allowing updates only within the editable region, while preserving the remainder of the grid as immutable conditioning context.